CONF-960401--38

SAND96-1280C

CAPILLARY STRESS IN MICROPOROUS THIN FILMS

J. Samuel*, A. J. Hurd*, C.J. Brinker*†, N.K Raman†; L. J. Douglas Frink††; F. van Swol††
Ceramic Processing Science Department, Sandia National Laboratories, Albuquerque, NM 87185-0609*; Department 9225, Sandia National Laboratories, Albuquerque, NM 87185-1111††, UNM-NSF Center for Micro engineered Ceramics, University of New Mexico, Albuquerque, NM 87131†

ABSTRACT

Development of capillary stress in porous xerogels, although ubiquitous, has not been systematically studied. We have used the beam bending technique to measure stress isotherms of microporous thin films prepared by a sol-gel route. The thin films were prepared on deformable silicon substrates which were then placed in a vacuum system. The automated measurement was carried out by monitoring the deflection of a laser reflected off the substrate while changing the overlying relative pressure of various solvents. The magnitude of the macroscopic bending stress was found to reach a value of 180 MPa at a relative pressure of methanol, P/Po = 0.001. The observed stress is determined by the pore size distribution and is an order of magnitude smaller in mesoporous thin films. Density Functional Theory (DFT) indicates that for the microporous materials, the stress at saturation is compressive and drops as the relative pressure is reduced.

INTRODUCTION

When a porous material is brought into contact with a vapor, condensation will take place at a vapor pressure lower than the bulk saturation vapor pressure[1]. This capillary condensation induces stress in the material[2]. Capillary stress may cause cracking[3] and is one of the factors in dictating the final structure of a porous material that results from a drying gel[4]. The tensile stress induced in large pores can be understood in terms of bulk thermodynamics through the Kelvin and Laplace equations. For microporous materials, with pore diameters of a few solvent molecules, assumptions underlying the bulk thermodynamic description are expected to break down[5].

We have used microporous thin films prepared by a sol-gel route to study capillary stress in extremely small pores. These materials have the advantage of molecular sized pores and narrow pore size distributions as witnessed by the molecular sieving capabilities of similarly prepared membranes[6]. The stress in these films was measured under reduced vapor pressure of condensable vapors using a beam bending technique[7]. Experimental results show a large difference in stress for a microporous film under saturation versus vacuum, for example in methanol this difference reaches a value of 220 MPa. In order to understand the origin of capillary stress in small pores we have used a non-local density functional theory approach[8]. The results indicate that for pores on the order of a few adsorbate molecules in diameter, packing constraints on the adsorbate cause stress at saturation to be compressive, thus the stress in microporous materials is qualitatively different from that seen in large pores, in that it goes from compressive at saturation to zero under vacuum.

EXPERIMENTAL

Sol Preparation and Deposition: Sols were prepared from tetraethoxysilane (TEOS), water and HCl or NH_4OH in a two step process. In the first step, a stirred solution of TEOS was partially hydrolyzed under reflux for 90 minutes (TEOS: ethanol: water: HCl ratio of 1: 3.8: 1: $7x10^{-4}$). In the second step of the preperation of the acid catalyzed sol, (A2), water, ethanol and acid were added to give a final TEOS: ethanol : water : HCl : Ratio of 1:19.6 : 5.1 : 0.056. For the B2 film, the second step entails adding water , NH_4OH and ethanol to give a final TEOS: ethanol: water: HCl: NH_4OH ratio of (1:21:3.7: 0.0007: 0.0009). The B2 sol was subsequently aged for 24 hours in a sealed container at 50°C. The films were deposited on 150μm thick <100> double polished silicon wafers by dip-coating in a dry atmosphere ([H_2O]~10ppm) at a speed of 1.7 mm/sec. The films were deposited on one side of the wafer by masking the opposite side with a layer of parafilm which was removed before heating the films to a temperature of 400 °C. The film thickness, measured by ellipsometry (Gartner L116C ellipsometer), was ~1000 Å. The films were

deposited, under identical conditions, on a 390μm thick double polished <100> silicon substrate which was then used for IR experiments.

Stress Measurement: The stress measurement is carried out using a beam bending or cantilever technique[3], [7]. The thin porous film is deposited on a substrate (beam) of known thickness and modulus and the amount of stress exerted by the film is found from the change in curvature of the beam. The thin films were deposited on one side of 150μ or 75μ <100> single crystal double polished silicon wafers. A sample with dimensions of approximately 1 cm width and 5 cm length was clamped in a vertical position in the vacuum chamber. The sample was pumped down to a pressure of 1e-5 torr. Pressure was measured with a series of stabilized MKS transducers (0.1, 10 and 100 torr full scale). A 6mw HeNe laser is passed through a x40 beam expander and iris to reduce divergence and is then bounced off the uncoated side of the sample. The beam is bounced between 4 mirrors and is detected at a position sensitive detector (UDT model SL15). The path length of the beam can be changed to accommodate different extents of deflection. The solvent, after being degassed by freeze thaw cycles, is dosed into the chamber through a needle valve. The dosing is automatically controlled and the pressure and the height of the reflected laser spot are stored in the computer after a predetermined equilibration time. The stress measurement may be run in a kinetic mode by abruptly changing the partial pressure over the sample and following the stress at 1 second intervals, or an isotherm may be automatically collected for a series of pressures.

The lateral deflection of the wafer, δ, at the point that the laser hits the sample, is related to the change in height of the laser spot on the detector, h, by $\delta = L\,h/(4P)$ where P is the pathlength from the sample to detector, and L is the cantilever length. Under conditions of small deflection and film thickness relative to substrate thickness, δ is related to the stress in the film, s, by Stoney's equation: $s = E_w\, d_w^2 / (3L^2\,(1-\nu_w)\, d_f)\,\delta$ where E_w is Young's modulus of the substrate, d_w is the substrate thickness, d_f is the film thickness and ν_w is the substrate Poisson ratio.

IR measurements: Infrared adsorption spectra were collected on a Nicolet 800 FTIR equipped with a vacuum cell. Spectroscopic determination gave us sufficient sensitivity to measure the small amounts adsorbed on the thin film (up to 0.84 μgrams/cm^2 at saturation). The sample under vacuum was used as a background and the spectra from 975 cm-1 to 4000 cm-1 were collected under controlled vapor pressure. The spectra were corrected for the vapor phase contribution using an uncoated wafer at similar pressures.

RESULTS AND DISCUSSION.

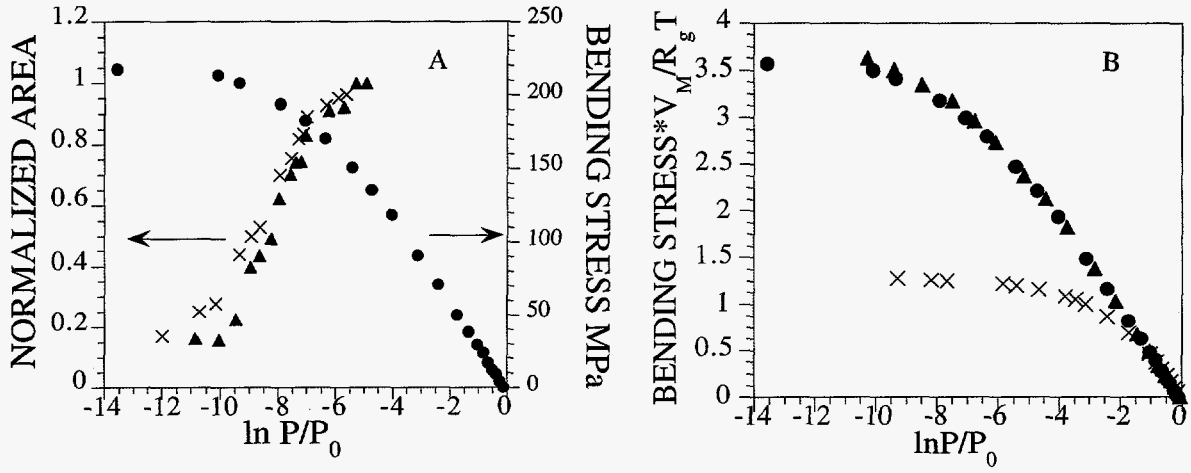

Figure 1: Adsorption and stress isotherms for an A2 film (pore diameter ~ 6 Å). **A:** Adsorption isotherm for methanol measured by FTIR (left axis) and stress isotherm (right axis); ▲ adsorption, x desorption, stress ● adsorption. The normalized amount adsorbed, plotted in the isotherm, is found from the peak area of 3600-2750 cm^{-1}, which encompasses a broad OH stretch band centered at 3330 cm-1 and CH_3 stretches at 2956.8 cm^{-1} and 2848.6 cm^{-1}. **B** stress isotherm for: ▲ acetonitrile, ● methanol, x water. The plots are scaled by V_m/R_gT, V_m is the molar volume, R_g is the molar gas constant and T the temperature.

Microporous films: In Figure 1A we compare the stress isotherm with the adsorption isotherm measured by FTIR spectroscopy. The most important feature is that the bulk of the change in stress takes place with no discernible change in the amount of methanol adsorbed. This means that the very appreciable stress induced in the film on altering P/P_0 is not simply a result of added adsorbate causing swelling but is a result of changes in the solvation force exerted by the adsorbate. For a series of adsorbed molecules, the initial part of the stress isotherm that is linear in $\ln(P/P_0)$ scales inversely with the molar volume of the adsorbate, V_m . This may be seen in Fig. 1B where we have plotted the stress isotherms of an A2 film for water , acetonitrile and methanol scaled by $V_m / R_g T$.

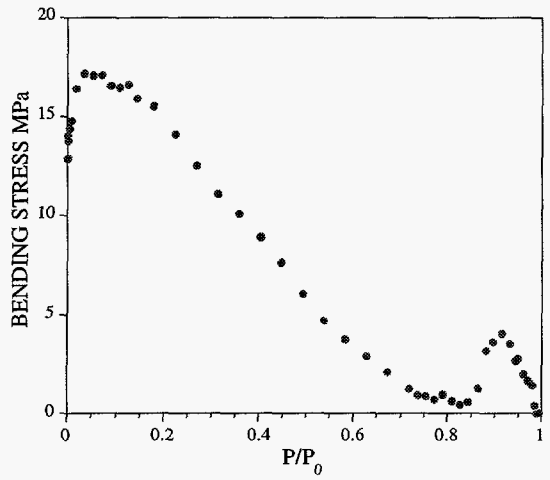

Figure 2 : Stress desorption isotherm measured for a mesoporous B2 film under methanol.

We determined the pore size of the microporous films by measuring the sieving behavior of the films towards a series of alcohols. the measurements were carried out by equilibrating the system at low P/P_O ($\sim 10^{-7}$) and observing the change in stress upon exposure (at $P/P_O = 0.8$) to a series of alcohols of increasing kinetic diameters. For methanol vapor (σ = 5.6 Å), the change occurred instantaneously, while for 2-propanol (σ = 7.6 Å), no change in stress was observed. For ethanol vapor (σ = 6.2 Å), the stress changed with a half-life of 180 minutes, establishing the average pore diameter as approximately that of an ethanol molecule. Both the extremely sharp isotherm (Figure 1A) and size exclusion experiments indicate molecular sized pores. The ultramicroporous nature, and narrow pore size distribution of the silica films used is further supported by the fact that a microporous silica thin film, similar to those used in this experiment, when deposited on a porous support, has been used as a membrane to separate nitrogen and oxygen[6].

Mesoporous Films: Base catalyzed xerogels (B2 gels) are characterized by a larger average pore diameter than that seen in the acid catalyzed gels[9]. The B2 gels are mesoporous and are characterized by type IV isotherms with average pore diameters in the 30-40 Å range.
The B2 film develops considerably lower stress than the microporous film, and the isotherm is not monotonic, there is a peak in the stress at $P/P_0 \sim 0.9$ and an additional drop in stress at $P/P_0 \sim 0.05$.

DISCUSSION

Capillary condensation under reduced relative pressure induces tensile stress[2]. For large enough pores, the Kelvin and Laplace equations yield the following equation[10]

$$s_{bend} \propto P_c = \gamma / r_m = -\ln(P/P_O)\, R_g T / V_m \qquad (1)$$

essentially this equation is a chemical potential equation, with the capillary stress P_c following the chemical potential. Comparing equation 1 to the experimental results we see that the ratio of the slopes for various solvents, on the same film, should be equal to the inverse ratio of the molar volumes, as is indeed observed experimentally.

What we measure in the experiment is the bending stress s_{bend}, this is related to the solvation induced stress by equation 2[11]:

$$s_{bend} = C_\upsilon \zeta P_c \qquad (2)$$

where υ is Poisson's ratio and $C_\upsilon = (1-2\upsilon)/(1-\upsilon)$[12]. C_υ stems from the biaxial nature of the stress developed due to attachment of the film to the substrate. For a typical value of $\upsilon = 0.2$ measured for a variety of silica gels, $C_\upsilon = 0.75$[12]. The parameter ζ for a saturated porous media is generally accepted to be $1- (K_n/K_S)$ [13] where K_n is the bulk modulus of the film and K_S is the bulk modulus of the silica skeleton. Based on the volume fraction porosity of the film (0.15 - 0.2, as measured by IR sorption and ellipsometry experiments) and literature data concerning the scaling of bulk modulus with porosity[14], we expect ζ to be in the range 0.4 -1. Comparing the predicted slope R_gT/V_m to the experimental slope in Figure 2b gives $C_\upsilon\zeta = 0.49$ and, using $C_\upsilon = 0.75$, $\zeta = 0.64$, well within the expected range

In the experiment, we measure the difference between the stress in the film at saturation and under vacuum. As the relative vapor pressure is reduced the force on the film becomes attractive but we know nothing about the absolute value of the stress at saturation. Attributing the results to capillary tension assumes that the stress is zero at saturation and becomes tensile as the pressure is reduced.

If the stress in the film is indeed caused by capillary tension induced by the adsorbate at reduced relative pressure this stress should relax under vacuum when desorption occurs, and a maximum in the absolute value of the stress should be seen. For microporous films this is not the case, the stress changes monotonicly with P/P_0. An additional question is raised by the magnitude of the stress change. The magnitude of the calculated tensile stress that the adsorbed fluid must exert in order to cause the measured bending stress is 380 MPa at $P/P_0 = 0.001$ (Equation 2). This is considerably beyond the predicted tensile strength of the bulk liquid[15],[10]. While the Kelvin approach assumes that the confined fluid has bulk properties at saturation, It is clear from surface force apparatus experiments that the characteristics of fluids confined in small dimensions differ greatly from bulk fluid characteristics[16]. Indeed, the density and solvation force of a fluid confined between to plates is seen to oscillate widely as a result of packing constraints.

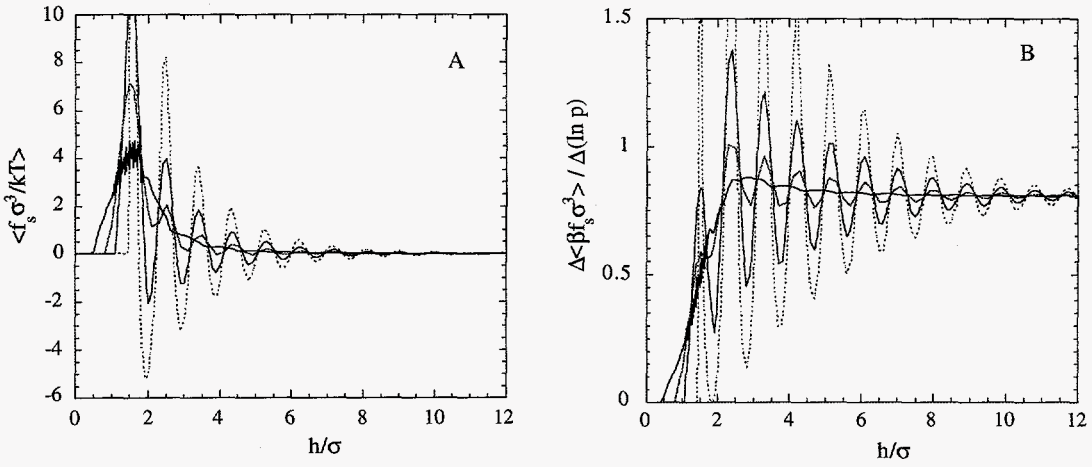

Figure 3: The solvation force (**A**) and the derivative of the solvation force with respect to lnP (B) for a saturated Lennard-Jones fluid in a slit pore obtained from DFT calculations. The dashed line is the result for monodisperse pores. The solid lines are the result for pores with a Gaussian distribution of pore sizes. In order of decreasing amplitude of oscillation these curves correspond to standard deviations of 0.2σ, 0.3σ, and 0.5σ. <h> is the slit width and T the temperature

In order to better understand the results, we have applied a non local density functional approach (DFT) [8]. The pores we consider are slits, and the fluid-fluid and fluid-wall interactions are characterized with 12-6 and 9-3 Lennard Jones potentials respectively. All potentials are cut and shifted at $r/\sigma = 10$ where pore sizes are characterized by the seperation between the walls, h/σ and

σ is the molecular diameter of the solvent. The ratio of the fluid-wall interactions (ε_{wf}) and fluid - fluid interactions (ε) are chosen to be $\varepsilon_{wf}/\varepsilon = 5.0$, where the fluid is wetting with a contact angle cos (θ) = 1[17]. In figure 3 we plot out the solvation force per unit area, f_s, (reduced by σ^3/kt) and the derivative of the solvation force with respect to ln P near saturation. f_s oscillates as a function of h/σ. This is a result of oscillations in the density caused by packing constraints at such small separations.

In real systems there is a certain amount of polydispersity. We imposed polydispersity on the DFT calculations by using a Gaussian distribution centered on h/σ with a standard deviation of γ. The oscillations in the solvation force are increasingly damped as the standard deviation is increased. Most importantly, polydispersity does not damp out solvation force to 0 and there remains a compressive force at saturation for γ=0.5 and $\langle h/\sigma \rangle < 4$ (Figure 1A).

The derivative of the force with respect to lnP may be seen in figure 3B. The derivative, which may be compared to the initial slope of the isotherms near P/P_0 =1, oscillates for the monodisperse pore system, and reaches the Kelvin result for large pores. When polydispersity is imposed the oscillations, which are nearly symmetric around the Kelvin value, are damped. As a result the slope is predicted to be within 20% of the Kevin value for a moderately polydisperse system pore system in which $h/\sigma > 1$.

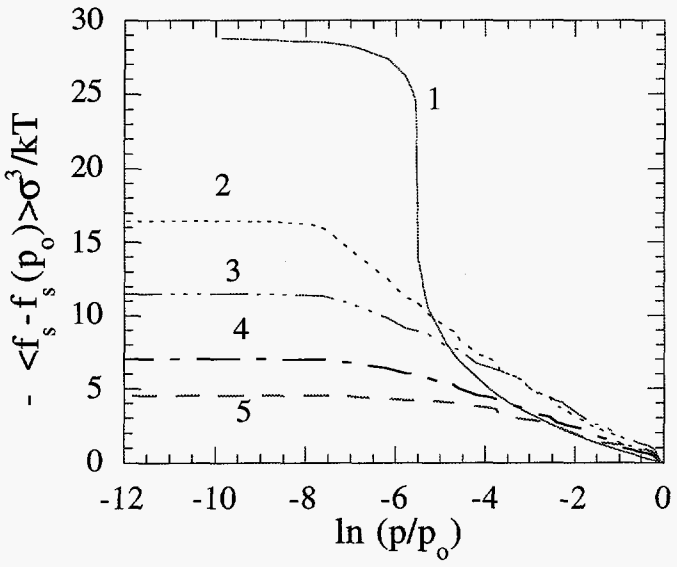

Figure 4: The solvation force as a function of relative pressure for an ensemble of pores characterized by Gaussian pore size distributions that differ primarily in their standard deviation . 1) γ =0, h =1.58; 2) γ =0.1, h =1.64; 3) γ =0.2, h =1.58; 4) γ =0.3, h =1.60; 5) γ =0.5, h =1.60;.

In Figure 4 we have plotted out an isotherm of the DFT result, i.e. the variation in solvation force as a function of pressure. These results may be compared to the experimental results in Figure 1B. In order to facilitate comparison, the DFT results have been shifted to 0 stress at saturation and $-f_s$ is plotted out versus ln P/P_0. The magnitude of the stress difference multiplied by σ^3 decreases as the standard deviation of h/σ decreases. This reduction is caused by a drop in the compressive force at saturation. The stress changes monotonicaly as $\ln P/P_0$ is reduced, leveling off at low P/P_0. comparing this to the experimental results in 1B, we see that a standard deviation of γ =0.3 maps reasonably well onto the experimental results. Methanol and acetonitrile, which have similar molecular diameters, (5.5 and 5.6Å respectively) show similar plots in figure 1B. Water, which has a smaller diameter (σ = 4.3Å) shows a smaller stress difference both because of the larger value of $\langle h/\sigma \rangle$ and correspondingly, the larger degree of polydispersity. Note that the stress in the experimental plot is the bending stress and should be multiplied by a factor of~2 (from equation 2) to compare with the DFT results.

For sufficiently large pores ($h/\sigma > 4$) we would expect capillary tension at reduced P/P_0. The full isotherm for the mesoporous film (Figure 2), may be explained by a bimodal pore size distribution. A bimodal distribution of pores would be reasonable in the B2 films, which are formed by colloidal compaction of fractal clusters that takes place during film deposition. At high relative pressures a peak in stress, at P/P_0 = 0.9, is caused by capillary tension and subsequent emptying of the large pores. At lower pressures, a subset of smaller pores dominates the isotherm, causing an increase in the observed stress difference. The additional peak observed at low P/P_0 may be attributed to a component of tensile stress in the small pores, that relaxes when they empty.

CONCLUSION

The magnitude of stress induced by solvation forces in microporous materials can be quite considerable. For a microporous film the difference in bending stress between the state in vacuo and under a saturated atmosphere of methanol reaches a value of 220 MPa. The magnitude of the induced stress is influenced both by pore size and pore size distribution. The stress is clearly not caused by swelling because of added amount of solvent in the pores, as the the adsorption takes place in the range of P/P_0 from vacuum to P/P_0=0.001 while %80 of the change in stress takes place 1 >P/P_0>0.001. The stress develops logarithmically as a function of P/P_0 and the stress induced by various solvents scales with the bulk molar volume of the solvent, as would be predicted from the Kelvin and Laplace equations. Comparing the experimental results to density functional theory of micropores we conclude that (1) For the small pore materials the solvation forces are compressive at saturation dropping monotonicaly to zero in vacuo (2) That the pore sizes are indeed in the range of a few solvent molecules in diameter (3) That for the slope given by V_m to be observed there must be a pore size distribution and that the relatively high final stress observed is an indication of a relatively narrow distribution.

ACKNOWLEDGMENTS

The authors thank Rich Cairncross for helpful discussions and Hongbin Yan and Thomas M. Niemczyk for the IR measurements. This work was supported by the U.S. Department of Energy Basic Energy Sciences Program, the University of New Mexico/National Science Foundation Center for Micro-Engineered Ceramics and the National Science Foundation Division of Chemical and Transport Systems (CTS9101658). Sandia National Laboratories is a U.S. DOE facility operated under contract number DE-AC04-94AL 85000.

REFERENCES

1. S.J. Gregg, K.S. W. Sing, Adsorption, Surface Area and Porosity (Academic Press 1982).
2. G W. Scherer; J. Am. Ceram . Soc, **73**, 3 (1990)
3. G.W. Scherer, D.M.Smith ; J. Non Cryst Solids **189** (1995).
4. J.H.L.Voncken, C. Lijzenga, K.P.Kumar, K. Keizer, A.J. Burggraaf, B.C. Bonekamp; J. Mat. Sci. **27**, 472-478 (1992).
5. R. Evans in Capillarity Today: Lecture Notes in Physics 386, edited by G Petre and A Sanfeld (publishers: Springer-Verlag 1990) pp. 62-76.
6. R. Sehegal, J.C. Huling, C.J. Brinker; Proceedings of the Third International Conference on Inorganic Membranes, edited by Y.H. ma,1995 pp. 85-93.
7. E.M. Corcoran, Journal of Paint Technology **41** 635 (1969).
8. Y. Rosenfeld, J. Chem. Phys., **98**, 8120 (1993)
9. S.S. Prakash, C.J. Brinker, A.J. Hurd; J. Non Cryst Solids, **190**, 264 (1995).
10. C.G.V. Burgess, D.H. Everett; J. Colloid. Interface Sci. **33**, 611 (1970).
11. R.A.Cairncross, P.R Schunk, K.S. Chen, S.S. Prakash, J. Samuel, A.J. Hurd, C.J. Brinker IS&T Proceedings (1996).
12. C.J. Brinker, G.W Scherer, SOL-GEL SCIENCE, (Academic Press 1990).
13. S.K.Garg, A. Nur ; J.Geophysical Research, **78** 5911-5921(1973).
14. H. Hidach, T. Woignier, J. Phalippou, G. W. Scherer; J Non. Cryst Solids, **121,** 202, (1990).
15. O.Kadlec, M.M. Dubinin; J. Colloid Interface Sci. **31**, 479 (1969).
16. J Klein, E Kumacheva; Science, **169**, 816 (1995).
17. F. van Swol, J. R. Henderson, Phys. Rev. A, **40**, 2567 (1989).

DISCLAIMER